Supporting information

Magnetic Marshmallows for Soft Robotics: Magneto-Mechanical Characterization and Application in Switchable Adhesion Structures

Maxime Bès[1], Samuel Lamont[2], Azadeh Dufour-Lamartinie[1,2], Jean-Claude Mancer[1], Ludovic Olanier[1], Jérôme Robert[3], Franck Vernerey[2], Artem Kovalenko[1]

1 – Laboratoire Sciences et Ingénierie de la Matière Molle, ESPCI Paris, PSL University, Sorbonne Université, CNRS, F-75005 Paris, France

2 – Department of Mechanical Engineering and Material Science & Engineering Program, University of Colorado at Boulder, Boulder, Colorado, USA.

3 – Institut de Physique et Chimie des Matériaux de Strasbourg, F-67200 Strasbourg, France

SI.A. Scanning electron microscopy images

As shown on SEM image on Figure SI.1, the NaCl crystals in the template have random orientations and pores between them. The air is replaced by a PDMS-Fe mixture under vacuum.

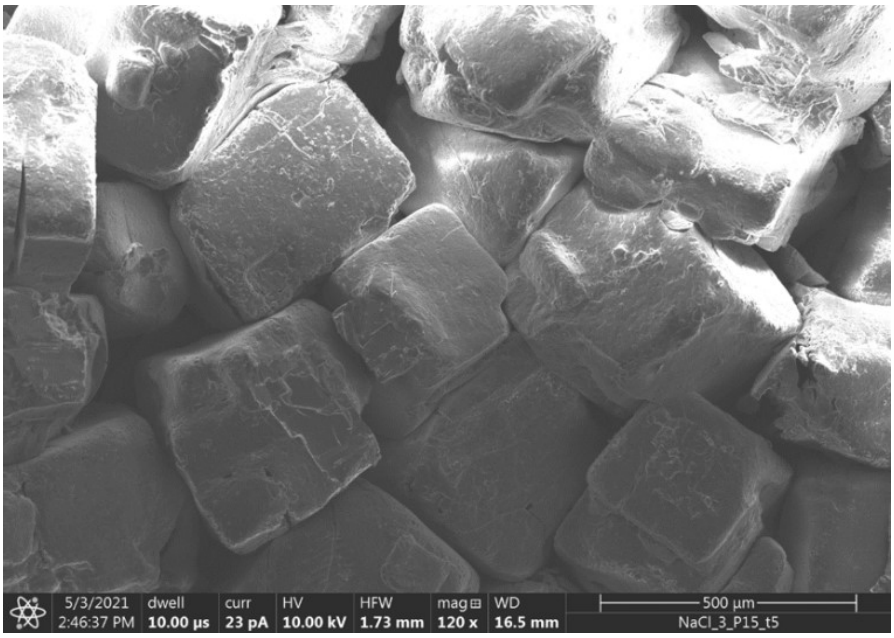

Figure SI. 1 – SEM of a fractured surface of a NaCl pellet template obtained at compaction pressure equal to 450 MPa.

Additional images of the internal structure of the foam F82.7-H6 are given on Figure SI.2. The images at low magnification show the irregular shapes of pore walls and openings between pores. The images at high magnification show the CIP distribution inside the matrix. The particles are slightly aggregated in clusters of variable shape without preferential orientation.

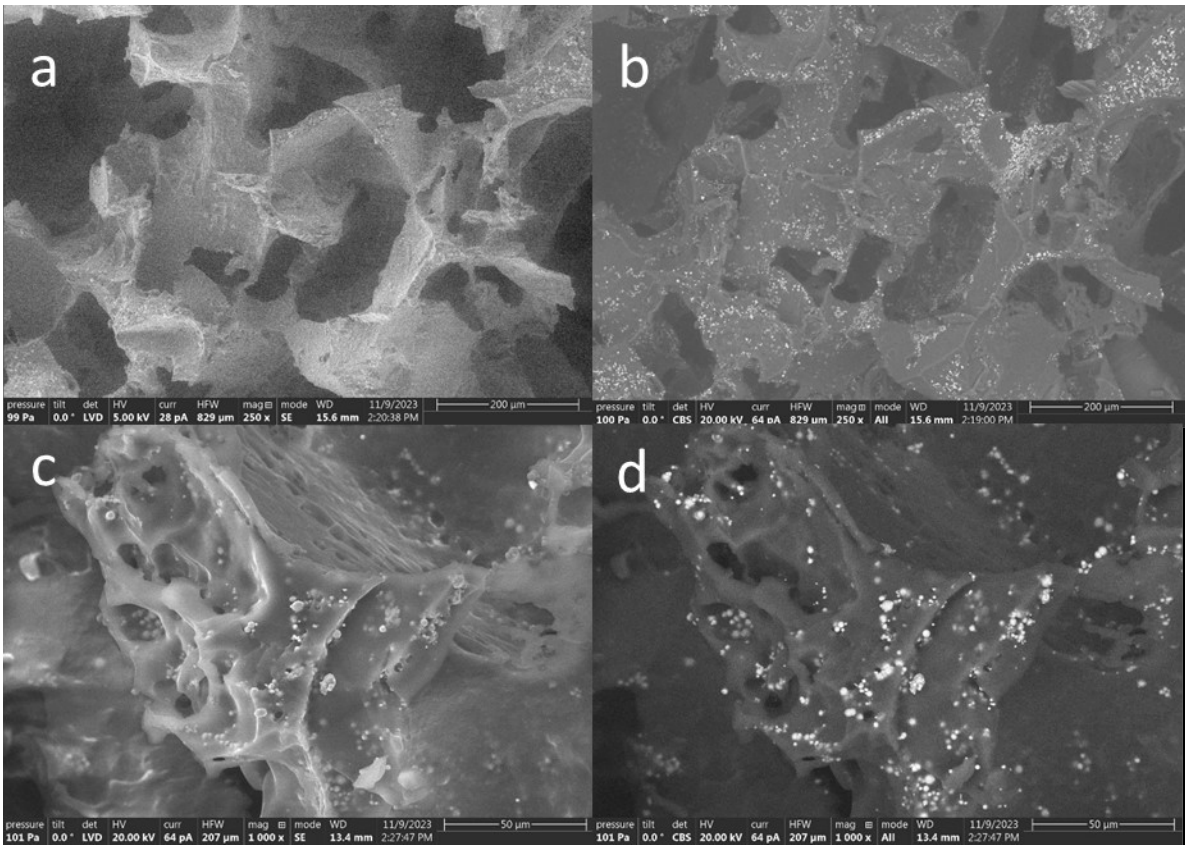

Figure SI. 2 – SEM images of the sample F82.7-H6 at low (a, b) and high (c, d) magnifications. The same zone of the sample was images using secondary electrons (a and c) or backscattered electrons (b and d).

SI.B. Magnetic measurements and computations

As shown in Figure SI.3, the saturation magnetization and mass susceptibility increase linearly with CIP mass fraction. This is expected for weakly interacting particles at low volume fractions.

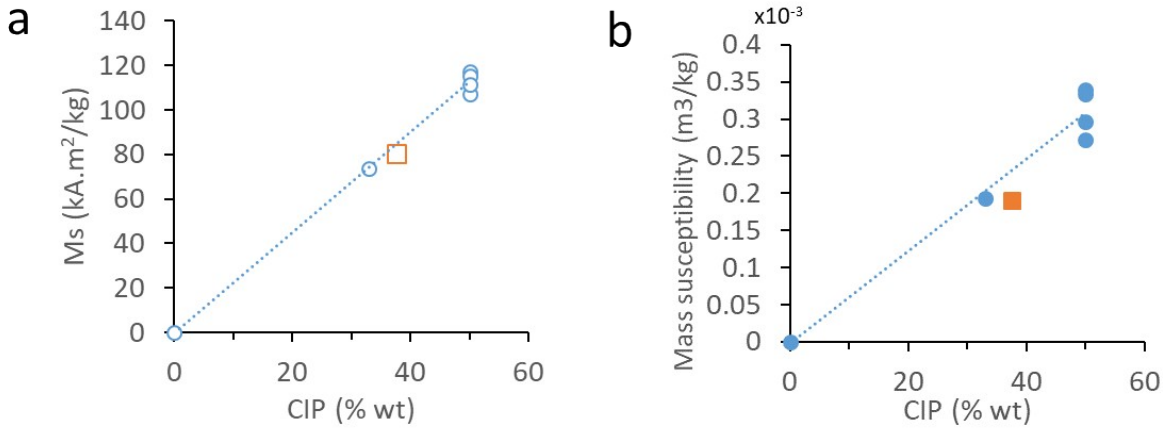

Figure SI. 3 – Saturation magnetization (a) and mass susceptibility (b) of magnetic PDMS samples (foams and non-porous samples) as a function of the mass fraction of CIP. The data in orange corresponds to a 37.8 %wt dispersion of CIP in inert hydrocarbon matrix (eicosane).

The magnetic force between the sample and the magnet was measured using the Instron tensile testing machine with a sample laying on a hollow clamp with a flat surface connected to the force sensor and a magnet fixed under the sample. The curves of the force as a function of the distance z between the upper surface of the magnet and the lower surface of the foam are shown on the Figure SI.4 (a, b). The shape of curves is very similar for all samples showing the decrease of the force with the distance. The higher attraction force for samples with lower porosity and large height is explained by higher iron mass in the sample. As consequence of the decrease of the force, the total height change ΔH_{mag} and total strain $\Delta H_{mag}/H_{initial}$ also decrease with the distance z as represented on Figure SI.4 (c and d).

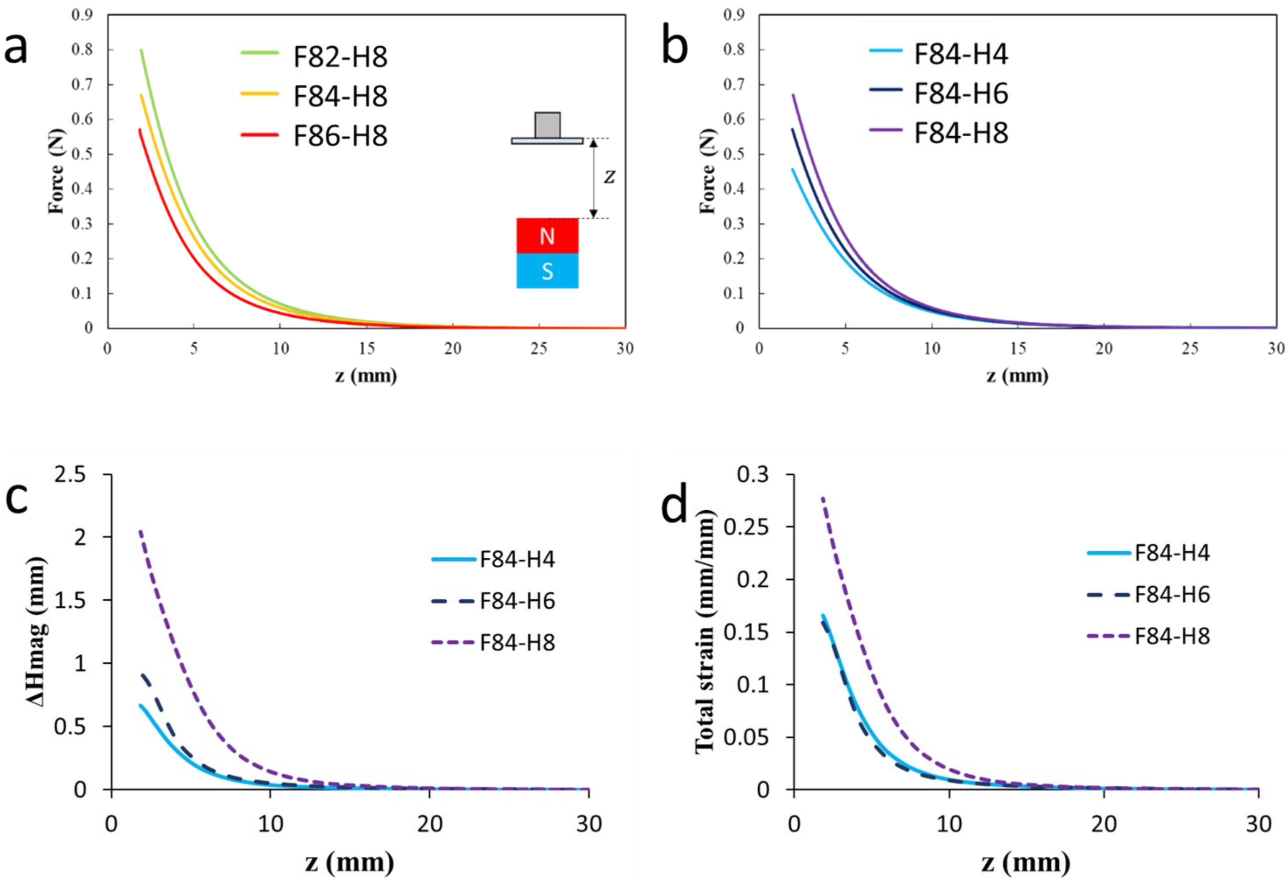

Figure SI. 4 – Magnetic force (a, b), total height change (c) and total strain for magnetic foams as a function of the distance between magnetic foam and a permanent magnet.

To select a magnet with most homogeneous distribution of the field in plane, we simulated the distribution of the vertical component of the field H_z around cylindrical magnets with fixed length L_{mag} = 20 mm and different diameters (Figure SI.5a) using an open source package Magpylib[1] implicated in Python. The curves on Figure SI.5b demonstrate that the optimum diameters corresponding to a sample with diameter of 13 mm are ranging from 15 to 20 mm. In the rest of the work, we choose the S20-20-N magnet from Supermagnete with diameter of 20 mm. Figures SI.5c and d show the spatial distribution, respectively, vertical and horizontal components of the field as a function of z and x coordinates.

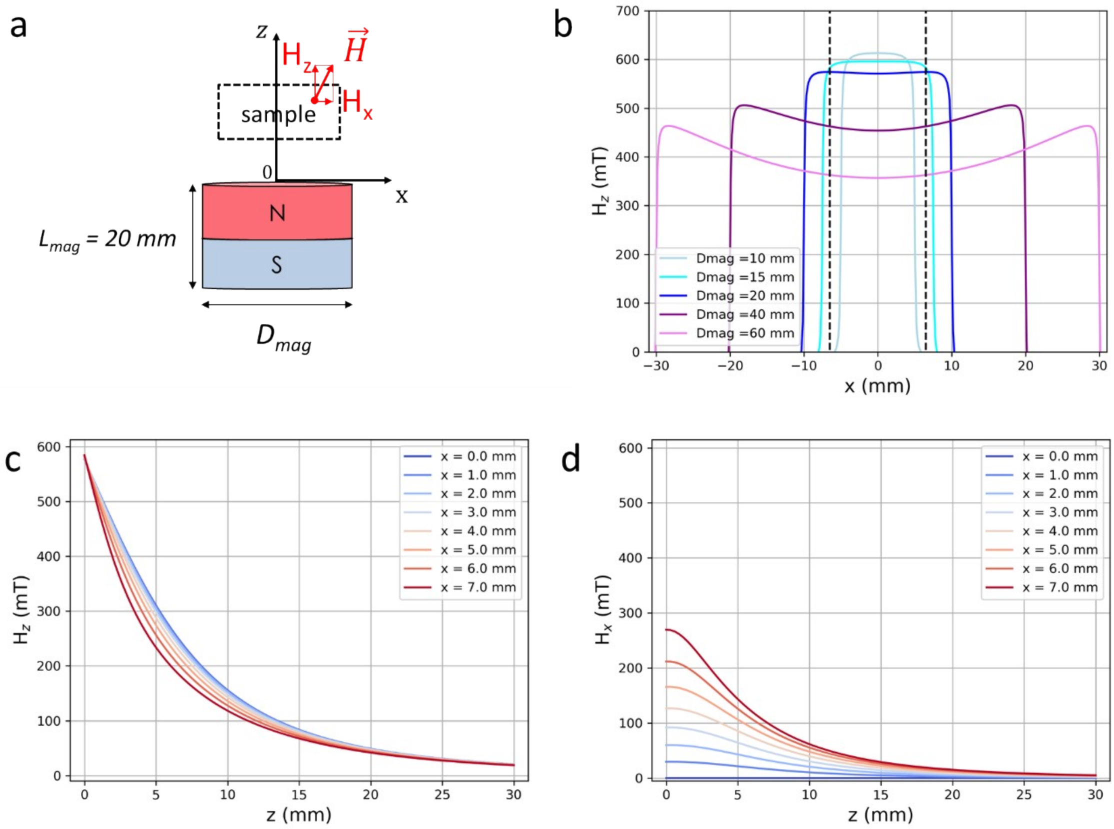

Figure SI. 5 – Simulated distribution of the magnetic field H near a cylindrical magnet (B_{rem} = 1.29 T) with fixed height L_{mag} = 20 mm: a) the sketch of the magnet; b) effect of the magnet diameter D_{mag} on the horizontal distribution of vertical field component H_z; c) dependence of the vertical component H_z on the coordinate z for different distances x from central axis of the magnet S20-20-N with D_{mag} = 20 mm; d) dependence of the horizontal component H_x on the coordinate z for different distances x from central axis of the magnet S20-20-N with D_{mag} = 20 mm.

The experimental values of H_z on the vertical axis of the magnet S20-20-N were measured with a MFM 3500 gaussmeter from PCE Iberica and showed a very good agreement with the computations (Figure SI.5).

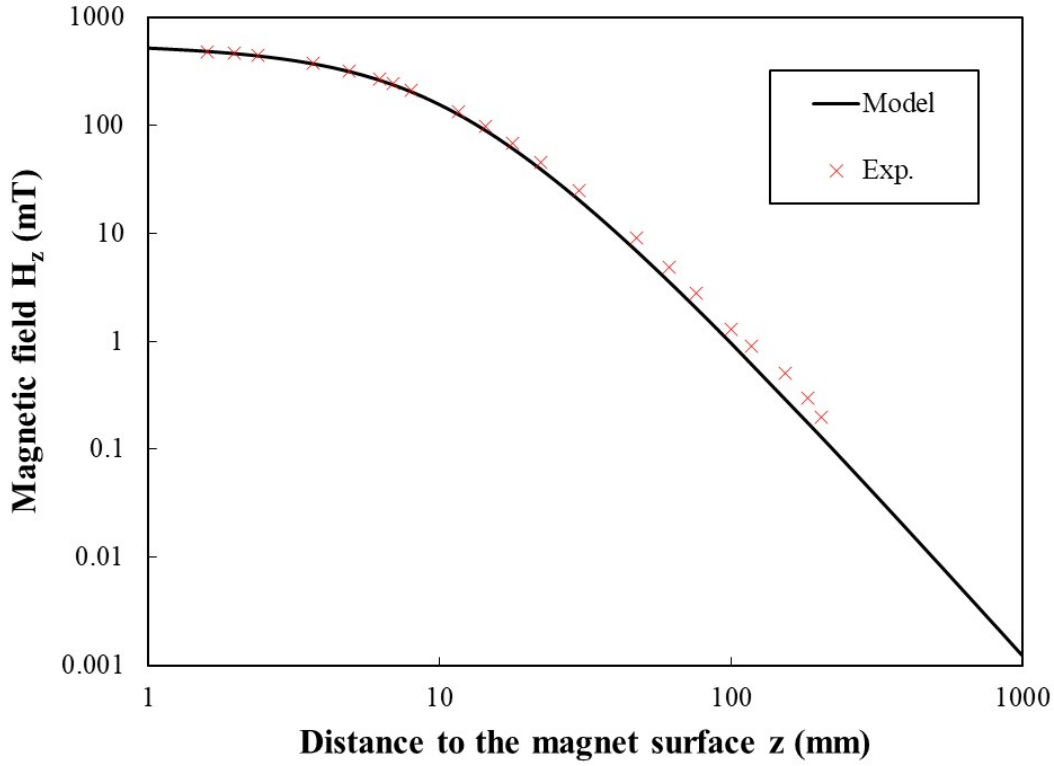

Figure SI. 6 – Distribution of the vertical component of magnetic field Hz at the central axis of the magnet S20-20-N as a function of the distance to the magnet surface.

SI.C. Samples' dimensions, porosities, mechanical and magnetic properties.

The following table gives the names of fabricated samples, the values of salt template relative densities $\rho_{pellet}/\rho_{NaCl}$, the final geometrical porosities Φ, as well as elastic compression moduli E and calculated magnetic susceptibilities χ.

Table SI.1.

Sample	$H_{initial}$ (mm)	$\rho_{pellet}/\rho_{NaCl}$	Φ §	E (kPa)	χ (dimensionless)
F82-H4	3.97	79.9	81.7	8.33	0.104‡
F82-H6	5.95	82.7	82.1	7.78	0.102‡
F82-H8	8.31	82.2	81.7	8.22	0.104‡
F84-H4	4.04	83.5	84.0	5.94	0.091‡
F84-H6	5.85	84.8	84.4	5.31	0.089‡
F84-H8	7.39	85.7	84.3	4.78	0.0896‡
F87-H4	3.74	87.3	87.0	3.17	0.074‡
F87-H6	5.62	86.5	85.9	3.93	0.080‡
F87-H8	7.96	87.4	87.2	3.15	0.073‡
PDMS-Fe	-	non-porous	non-porous	775 kPa	0.481

§ - porosity calculated from mass (m_s), volume (V_s) of the sample using equation $\Phi = m_s/(V_s \cdot \rho_{PDMS-Fe})$ where $\rho_{PDMS-Fe}$ = 1767 kg/m^3 is the theoretical density of the matrix.

‡ - volumetric magnetic susceptibility calculated from the mass susceptibility of foams χ_g = 0.0002723 m^3/kg and porosity using equation: $\chi = \chi_g \cdot \rho_{PDMS-Fe} \cdot (1 - \Phi)$

SI.D. Analytical modelling of magnet-foam interactions

The magnetic field $H(z)$ along the axis of a cylindrical magnet with remanent magnetization B_{rem} (in units of Tesla) and dimensions L_{mag} and R_{mag} can be described by equation:

$$H(z) = \frac{B_{rem}}{2\mu_0}\left(\frac{z + L_{mag}}{\sqrt{(z + L_{mag})^2 + R_{mag}^2}} - \frac{z}{\sqrt{z^2 + R_{mag}^2}}\right) \qquad (SI.1)$$

Close to the magnet, the field can be considered as linear function of the distance:

$$H(z) \approx \frac{B_{rem}}{2\mu_0}\left(\frac{1}{\sqrt{1 + \left(\frac{R_{mag}}{L_{mag}}\right)^2}} - \frac{z}{R_{mag}}\right) = \frac{B_{rem}}{2\mu_0}(b - az) \qquad (SI.2)$$

Where coefficients are a = $1/R_{mag}$ and $b = \left[1 + \left(\frac{R_{mag}}{L_{mag}}\right)^2\right]^{-0.5}$. In this case, the slope of the magnetic field is a constant:

$$gradH(z) = -\frac{aB_{rem}}{2\mu_0} \qquad (SI.3)$$

The attraction body force f_{mag} (in N/m^3) that acts on a material with magnetic susceptibility χ may be approximated as:

$$|f_{mag}| \approx \mu_0 \chi H_z \cdot \frac{dH_z}{dz} \approx \frac{a\chi B_{rem}^2}{4\mu_0}(b - az) \qquad (SI.4)$$

equilibrium equation for the deformed configuration:

$$d\sigma = f_{mag}dz$$

With limit conditions: σ (z=$H_{initial}$) = 0; u (z=0) = 0.

In assumption of small deformations $\Delta H_{mag} \ll H_{initial}$, the integration may be done in the reference configuration:

$$\sigma(z) \approx \frac{a\chi B_{rem}^2}{4\mu_0}\int_0^z (b - az)\, dz = \frac{a\chi B_{rem}^2}{8\mu_0} z(2b - az) + Const$$

$$\sigma(H_{initial}) = 0$$

$$Const = \sigma(0) = -\frac{a\chi B_{rem}^{2}}{8\mu_0} H_{initial}(2b - aH_{initial})$$

$$\sigma(z) = \frac{a\chi B_{rem}^{2}}{8\mu_0}(z - H_{initial})(2b - a(z + H_{initial}))$$

If we apply a linear elastic behavior (Hookes's law in compression):

$$\sigma(z) = E\varepsilon(z)$$

The height change may be obtained by integrating the strain along the sample:

$$\Delta H_{mag} = \int_0^{H_0} \varepsilon(z)dz = \frac{a\chi B_{rem}^{2}}{8E\mu_0} H_{initial}^{2}\left(\frac{2a}{3}H_{initial} - b\right) \; (SI.5)$$

SI.E. Numerical modeling for large strains

In the numerical model, we consider a finite-strain continuum formulation of the problem, which is governed by the balance of linear momentum. As there is negligible Poisson's effect, we may parameterize the motion of the foam by the position $z \in \Omega$ of a material point, where $\Omega \subset R^1$ is the domain occupied by the foam in the current configuration. In general, we seek to determine the mapping $z = \zeta(Z)$, which is a one-to-one function that captures the motion ζ of a material point initially at $Z \in \Omega_0$ of the reference domain to its current position z. Meanwhile, the stretch ratio $\lambda = \partial\zeta\partial Z$ represents the deformation of line elements between Ω_0 and Ω. In 1D, the balance of linear momentum is written:

$$\int_\Omega \left(\frac{\partial\sigma}{\partial z} + b(z)\right)dz = 0 \quad (SI.6)$$

Where $\sigma(z)$ is the Cauchy stress and $b(z)$ is the body force per unit volume. In this problem, we may determine the body force as the equivalent force per unit volume that is acting on the foam due to the applied magnetic field. The magnitude of this force in 1D is written:

$$b(z) = \mu_0 \chi^{Fe} \rho^{Fe}(z) H(z) \frac{\partial H}{\partial z} \; (SI.7)$$

Where $\rho^{Fe}(z)$ is the mass density of iron particles, μ_0 is the permittivity of free space, and χ^{Fe} is the magnetic susceptibility (a property of the magnetic particles). In the numerical model, we use the exact representation of the magnetic field $H(z)$ given in Eq. SI 1. Note that while the cylinder deforms, the density of iron particles increases according to the change in volume $J(z)$ of the material point. Assuming that there is no Poisson's effect, the current density field may be written in terms of the original density field $\rho_0^{Fe}(z)$ as:

$$\rho^{Fe}(z) = \frac{1}{\lambda} \rho_0^{Fe}(z) \;\; (SI.8)$$

In practice, we assume that the original density field ρ_0 is constant across the sample. The typical value of this quantity is 100-200 $kg\ m^{-3}$ in our foams. Finally, to complete the numerical model, we must propose a constitutive equation that links the deformation field to the stress field. As a first order approximation, we consider a simple linear elastic law:

$$\sigma(z) = E\epsilon(z), \quad with \quad \epsilon(z) = \frac{1}{2} - \frac{1}{4\lambda^2} \;\; (SI.9)$$

Here, $\epsilon(z)$ is the Euler-Almansi strain. To solve this system, we consider an Eulerian discretization of the domain Ω and solve Eq. SI.6 using the Finite Element Method in the weak form interface of COMSOL Multiphysics. Thus, we consider the localized balance equation and derive the weak form of Eq. SI.6 as:

$$\int_{\Omega} \left(\frac{\partial(\delta z)}{\partial z} \sigma(z) - (\delta z) b(z) \right) dz = 0 \;\; (SI.10)$$

Here, δz are the test functions, which represent virtual displacements of z. To obtain consistent boundary conditions, we ramp the magnetization constant χ from 0 to its true value over a finite time interval and solve Eq. SI.10 iteratively while neglecting inertial effects. After the simulation is complete, the final stress field $\sigma(z)$ and stretch field $\lambda(z)$ may be obtained by post-processing at the final timestep.

SE.F. Strain distribution

As shown in Figure SI.6, the numerical model better predicts the experimentally observed local strain in the sample as compared to its analytical counterpart. This leads to the overestimation of the total strain by the analytical model.

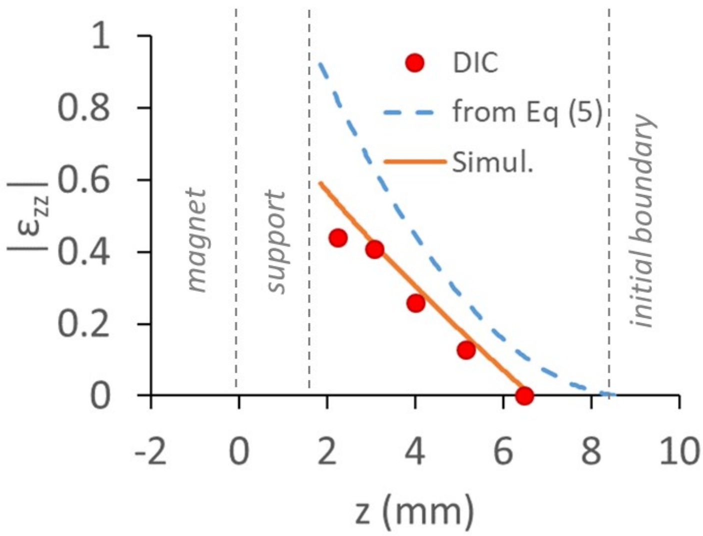

Figure SI. 7 - The predicted and experimental strain distribution inside the foam F84-H8 in its deformed state as a function of the vertical coordinate

SI.F. Adhesive and elastic properties of Sylgard184-Sylgard 527 mixtures.

The adhesive properties of the cured soft PDMS were characterized using a probe-tack test with a plane-plane geometry of diameter of 23 mm. The pull-off curves are represented in Figure SI.7. The failure was cohesive for S527 sample and adhesive for all other compositions. For the adhesion tests, we selected the composition 10%S184-90%S527 with a maximum tack stress $\sigma_{tack} \approx 4N/(23mm)^2 \approx 8\ kPa$ and the adhesion energy (integral of the pull-off curve) of 3 J m^{-2}. The mixture of two Sylgard grades at 25%S184-75%S527 weight ratio was used to make a sufficiently soft but not too sticky PDMS matrix (such as Sylgard 527).

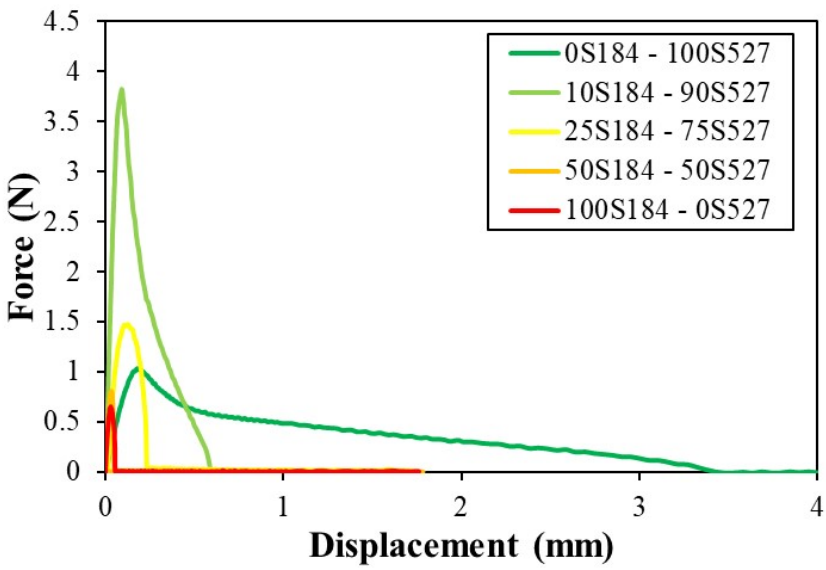

Figure SI. 8 – Pull-off curves of Sylgard 184 and Sylgard 527 mixtures for different mixing ratios

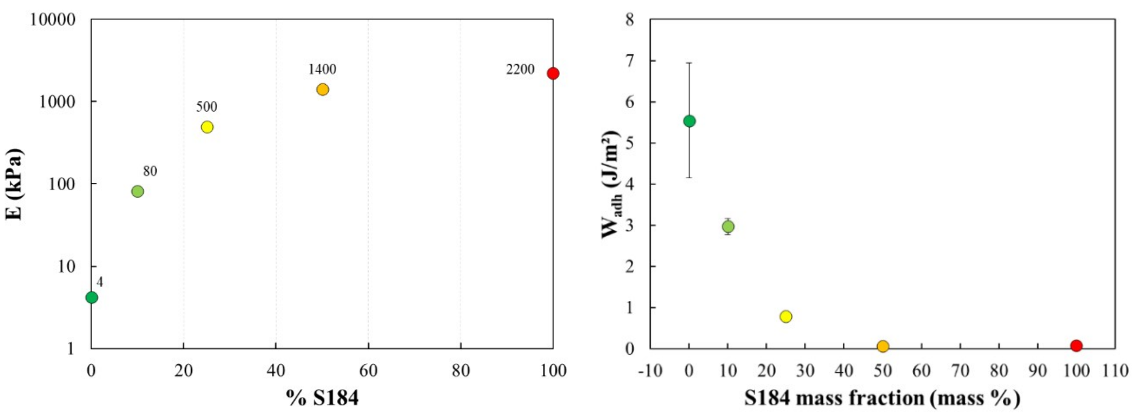

Figure SI. 9 – Compression modulus and adhesion energies as a function of Sylgard 184 and Sylgard 527 as a function of Sylgard 184 content.

References:

(1) Ortner, M.; Coliado Bandeira, L. G. Magpylib: A Free Python Package for Magnetic Field Computation. *SoftwareX* **2020**, *11*, 100466. https://doi.org/10.1016/j.softx.2020.100466.